

Optical model analysis of ^{12}Be and ^{14}Be quasielastic scattering on a ^{12}C target at 56 MeV per nucleon

Michel C. Mermaz

*Commissariat à l'Energie Atomique, Service de Physique Nucléaire, Centre d'Etudes de Saclay,
91191 Gif-sur-Yvette, Cedex, France*

(Received 25 April 1994)

An optical model analysis of the quasielastic scattering of ^{12}Be and ^{14}Be on ^{12}C target nuclei has been performed, for measurements at 679 and 796 MeV laboratory incident energy, respectively. The data are from the group of the University of Notre Dame. The automatic searches on the optical model parameters were constrained by fitting the total reaction cross sections to values extrapolated from measurements performed at much higher incident energy. It has turned out for both projectiles that a surface term is necessary for the real as well as for the imaginary part of the potential, in order to reproduce correctly the experimental data. This diffractive-refractive behavior favors the existence of a neutron halo for both projectiles.

PACS number(s): 24.10.Ht, 25.60.+v, 25.70.Bc

In this paper, we shall present an optical model analysis of the experimental data of Ref. [1], concerning ^{12}Be and ^{14}Be quasielastic scattering from a ^{12}C target. These data are well reproduced with a standard volume Woods-Saxon potential shape plus a surface term (normalized derivative of a Woods-Saxon shape) for the real as well as for the imaginary part. This work is in the same vein as the one already published for quasielastic scattering of ^{11}Li and ^{11}C on a ^{12}C target in the same incident energy domain [2]. One aim of this paper is to show that it is possible to reproduce the experimental elastic angular distributions with reasonable values for the total reaction cross sections. That was not the case for the optical model analysis of Ref. [1] where anomalously large reaction cross sections were obtained. It would be highly desirable to measure independently, by the attenuation method, total reaction cross sections at this 56 MeV per nucleon incident energies.

The difficulty in this analysis is that the data present large error bars due to the very weak intensities of such secondary radioactive nuclear beams. This can be circumvented by fitting at the same time the corresponding total reaction cross sections. These latter quantities, measured at high energy, are extrapolated towards the low-energy side using the semiclassical relationship [3]

$$\sigma_R = \pi R^2 \left(1 - \frac{V_C}{E_{c.m.}} \right),$$

where σ_R is the reaction cross section in fm^2 , $E_{c.m.}$ the center-of-mass energy, and V_C the height of the Coulomb barrier given by

$$V_C = 1.44zZ/R,$$

where z and Z are the projectile and target charges, respectively, and R the strong absorption radius. This formula of σ_R is more obvious than the one used in Ref. [1].

At 790 MeV per nucleon the reaction cross sections of ^{12}Be and ^{14}Be are 927 and 1139 mb, respectively, from

the experiment of Tanihata *et al.* [4], leading to values of 911 and of 1122 mb, at 56 MeV per nucleon incident energy. These two values are much smaller than the 1238 and 1900 mb found for ^{12}Be and ^{14}Be , respectively, in the previous optical model analysis of Ref. [1], and more in agreement with what is already known for light systems from Refs. [2] and [5] at these low incident energies.

Due to the poor experimental energy resolution, inelastic cross sections to the first 2^+ and the first 3^- states of ^{12}C are not separated from the pure elastic cross section. Using the automatic search code ECIS88 of Raynal [6], it has been possible to fit this global elastic cross section by calculating the distorted wave Born approximation (DWBA) cross sections to the 4.439 MeV 2^+ and 9.641 MeV 3^- of ^{12}C and by adding them to g.s. elastic cross section before computing the χ^2 value used by the automatic search routine. It is well known that in case of heavy-ion scattering the DWBA reproduces rather well the inelastic scattering data in shape and magnitude [7]. The deformation parameters β_2 and β_3 are 0.592 and 0.400, respectively, coming from Refs. [8] and [9].

Figures 1 and 2 present the global elastic scattering best fits of the ^{12}Be and of the ^{14}Be on ^{12}C data, respectively, using volume Woods-Saxon shapes plus surface terms (normalized derivative of Woods-Saxon volume terms) for both real and imaginary potentials. The corresponding optical model parameters are given in Table I, family VS1 and VS2, assuming the same Coulomb field for both projectiles. In order to force the fits to go through all the data points, we have used for all of them a standard relative error bar of 10%. The χ^2 per point are 1.9 and 0.96 for ^{12}Be and ^{14}Be , respectively. The experimental error bars are in fact much larger for some points, see Ref. [1]. The corresponding total reaction cross sections, 911 and 1123 mb for ^{12}Be and ^{14}Be , respectively, fit extremely well the experimentally extrapolated cross sections.

In order to understand the obtained optical model potentials (12 parameters), we have plotted in Figs. 3 and 4 their shape for ^{12}Be and ^{14}Be , respectively. The puzzling

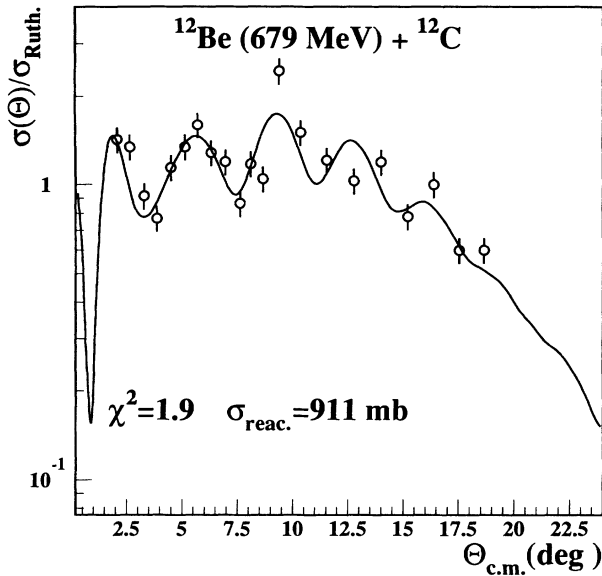


FIG. 1. Experimental angular distribution of the summed cross sections for ^{12}Be elastic scattering and inelastic scatterings to the first 2^+ and first 3^- states of ^{12}C target [1]. The solid line is the result of an optical model plus DWBA fit corresponding to family VS1 of Table I.

point of the data of Ref. [1] is that the elastic angular distribution for ^{12}Be is more far side dominated than the one of ^{14}Be projectile. That can be observed from the fact that at forward angles, in Fig. 1, the experimental points are higher and above the Rutherford values than the ones of Fig. 2. Thus, the real part of the ^{12}Be potential is of

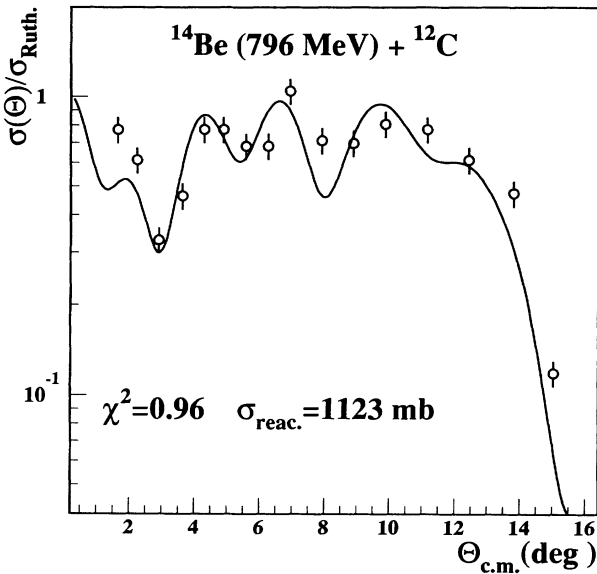


FIG. 2. Experimental angular distribution of the summed cross sections for ^{14}Be elastic scattering and inelastic scatterings to the first 2^+ and 3^- states of ^{12}C target [1]. The solid line is the result of an optical model plus DWBA fit corresponding to family VS2 of Table I.

TABLE I. Optical model parameters for ^{12}Be and ^{14}Be projectiles on a ^{12}C target. The χ^2 per point values correspond to standard relative error bars of 10%. The reduced Coulomb radius is equal to 0.924 fm for both projectiles.

Projectile	^{12}Be	^{14}Be
E_{lab} (MeV)	679.0	796.0
Potential family	VS1	VS2
V (MeV)	20.00	20.00
r_0 (fm)	0.924	0.702
a_0 (fm)	2.466	0.560
W (MeV)	6.83	5.44
r_i (fm)	0.683	0.762
a_i (fm)	1.261	0.146
V_s (MeV)	4.99	0.758
r_{0s} (fm)	1.115	1.817
a_{0s} (fm)	0.843	0.531
W_s (MeV)	7.94	4.24
r_{is} (fm)	1.046	1.323
a_{is} (fm)	0.366	0.597
σ_R (mb)	911	1123
σ_{2^+} (mb)	29.1	10.1
σ_{3^-} (mb)	10.8	4.1
χ^2	1.9	0.96

much longer range than that of ^{14}Be . Furthermore, in the case of the ^{12}Be projectile, a strong pocket is present in both the real and the imaginary parts of the potential near the nuclear surface while for the ^{14}Be projectile, this pocket shows up only in the imaginary part and far away from the nuclear surface. It is the imaginary part which is mainly responsible of the value of the reaction cross section and thus of the intensity of the nuclear halo. The pocket in the imaginary part is responsible of the neutron breakup cross section of the projectile. The last neutron-pair binding energies are 3.67 MeV for ^{12}Be [10] and 1.48 MeV for ^{14}Be [11]. Consequently the breakup

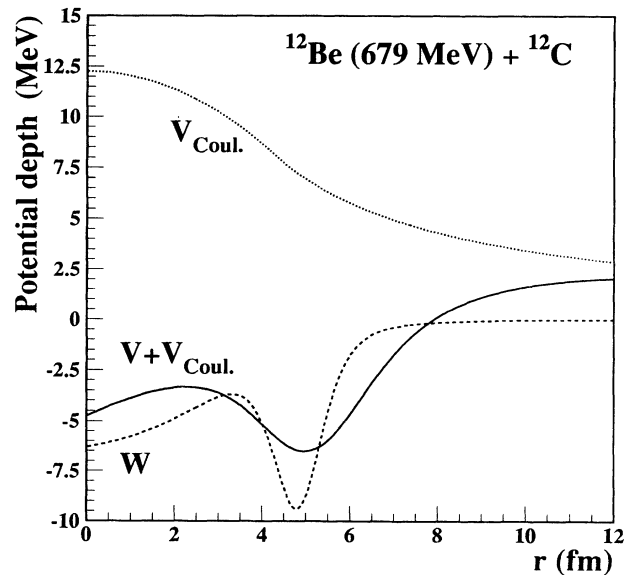


FIG. 3. The ^{12}Be optical model potential: volume term plus surface term family VS1 of Table I.

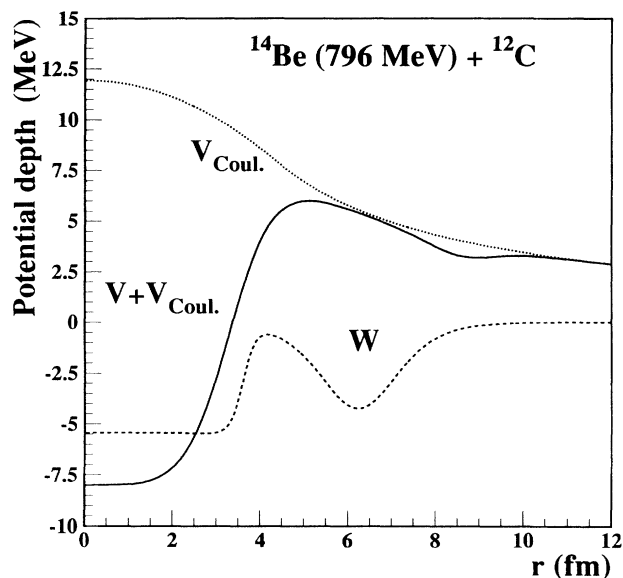


FIG. 4. The ^{14}Be optical model potential: volume term plus surface term family VS2 of Table I.

cross section has to be more stronger and more surface peaked for ^{14}Be nuclei. Furthermore, the ^{14}Be nucleus can be also considered as a ^{10}Be core surrounded by a cluster of 4 neutrons. This behavior can be qualitatively understood from Fig. 5 where are plotted the radial wave functions of the neutron pair for both projectiles along with the radial wave function of the four neutrons of ^{14}Be nucleus assuming a crude shell model filling for the neutrons. A reduced radius of 1.20 fm and a diffusivity of 0.65 fm were taken for all the bound state Woods-Saxon potentials. The binding energy of the four neutrons is 5.15 MeV. The last neutron pair of ^{14}Be belongs to the $2s-1d$ shell while the last neutron pair of ^{12}Be would belong more to the $1p$ shell, nevertheless the ^{11}Be ground state has already a spin $2s_{1/2}^+$. Thus, the former pair wave function has two nodes while the latter one has only one node. In the case of ^{14}Be projectile, the four-neutron wave function has three nodes: the large number of nodes favors also the existence of a neutron halo.

Using the total reaction cross section of Tanihata *et al.* [4], the strong absorption radii for ^{12}Be and ^{14}Be projectiles are 5.44 and 6.03 fm, respectively, well explained by the relative position of the pockets in the imaginary

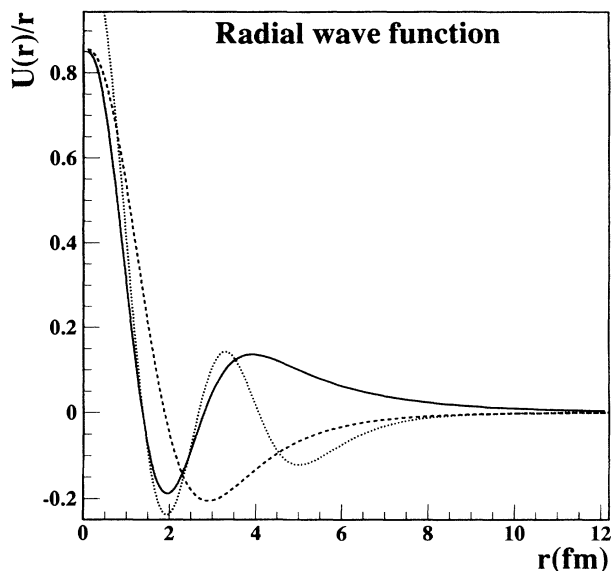


FIG. 5. The ^{14}Be and ^{12}Be two-neutron wave functions, solid curve and dashed curve, respectively. The dotted curve is the four-neutron wave function of ^{14}Be nucleus. The Woods-Saxon depths of the two-neutron bound state potentials are 45.72 and 78.97 MeV, respectively while the depth is 49.00 MeV for the four-neutron bound state potential. A reduced radius of 1.20 fm and a diffusivity of 0.65 fm were used in all the cases.

potentials of Figs. 3 and 4 and also by the wave function tails plotted in Fig. 5. It is a little bit puzzling to note from Figs. 3 and 4 that the real part of the optical potential is more refractive for the ^{12}Be nucleus than for the ^{14}Be nucleus.

The most important point before concluding is that, in the absence of high quality elastic scattering data with good energy resolution, it is necessary for the optical model parameter search to use the total reaction cross section as an input. It has turned out for both projectiles that the fitted optical model potentials have a long surface tail for the real and/or imaginary parts, which is compatible with the existence of a nuclear halo, the breakup feature being the stronger for ^{14}Be projectiles.

It is a pleasure to thank Professor Jacques Raynal from the Centre d'Etudes de Saclay for his help concerning his code ECIS88.

- [1] M. Zahar, M. Belbot, J. J. Kolata, K. Lamkin, R. Thompson, J. H. Kelley, R. A. Kryger, D. J. Morrissey, N. A. Orr, B. M. Sherril, J. A. Winger, and A. H. Wuosmaa, *Phys. Rev. C* **49**, 1540 (1994).
- [2] Michel C. Mermaz, *Phys. Rev. C* **47**, 2213 (1993).
- [3] Reiner Bass, *Nuclear Reactions with Heavy-Ions, Texts and Monographs in Physics* (Springer-Verlag, Berlin, 1980), p. 15.
- [4] I. Tanihata, T. Kobayashi, O. Yamakawa, S. Shimoura, K. Ekuni, K. Sugimoto, N. Takahashi, T. Shimoda, and

- H. Sato, *Phys. Lett. B* **206**, 592 (1988); I. Tanihata, H. Hamagaki, O. Hashimoto, Y. Shida, N. Yoshikawa, K. Sugimoto, O. Yamakawa, T. Kobayashi, and N. Takahashi, *Phys. Rev. Lett.* **55**, 2676 (1985).
- [5] B. Blank, J.-J. Gaimard, H. Geissel, K.-H. Schmidt, H. Stelzer, K. Sümmerer, D. Bazin, R. Del Moral, J. P. Dufour, A. Fleury, F. Hubert, H.-G. Clerc, and M. Steiner, *Nucl. Phys. A* **555**, 408 (1993).
- [6] J. Raynal, *Applied Nuclear Theory and Nuclear Model Calculations for Nuclear Technology Applications*, edited

- by M. K. Mehta and J. J. Schmidt (World Scientific, Singapore, 1988), p. 506.
- [7] P. E. Hodgson, *Nuclear Heavy-Ion Reactions* (Clarendon, Oxford, 1978), p. 260.
- [8] S. Raman, C. H. Malarkey, W. T. Milner, C. W. Nestor, Jr., and P. H. Stelson, *At. Data Nucl. Data Tables* **36**, 19 (1987).
- [9] R. H. Spear, *At. Data Nucl. Data Tables* **42**, 81 (1989).
- [10] A. H. Wapstra and K. Boss, *At. Data Nucl. Data Tables* **19**, 175 (1977); A. H. Wapstra, G. Audi, and R. Hoekstra, *ibid.* **39**, 281 (1988).
- [11] J. M. Wouters, R. H. Kraus, Jr., D. J. Vieira, G. W. Butler, and K. E. G. Löbner, *Z. Phys. A* **331**, 229 (1988).